Biomaterials Translational

Preclinical evaluation of aligned fibrin nanofibre hydrogels in a non-human primate model of spinal cord injury: A pilot study

Jia Yang[1#], Weitao Man[2#], Kaiyuan Yang[2#], Zheng Cao[1,3], Chao Ma[4], Kunkoo Kim[1], Zhe Meng[2], Yaosai Liu[2], Yuzhe Ying[2], Jie Zhang[2], Zide Wang[2], Yang Lu[2], Xiaolei Zhang[2], Guihuai Wang[2*] and Xiumei Wang[1*]

ABSTRACT

Spinal cord injury (SCI) often leads to partial or complete loss of motor, sensory, and autonomic functions. We have previously shown that the transplantation of hierarchically aligned fibrin nanofibre hydrogel scaffolds (AFGs) facilitates robust neuroregeneration and functional recovery in rat and dog SCI models. Given these positive results, we aimed to evaluate the biosafety and efficacy of AFGs in a non-human primate SCI model before exploring its potential in the clinic. In the present study, no significant adverse reactions were observed over 24 weeks following AFG implantation into 1-cm gaps in the hemisected thoracic spinal cords of monkeys (Macaca fascicularis). Scaffold implantation also reduced cystic cavity formation and encouraged axonal sprouting across the lesion site. Notably, detailed histological analysis demonstrated that AFG promoted high-density, sequential, and aligned nerve fibre regeneration, resulting in remyelination and vascularisation, ultimately leading to remarkable motor function recovery. These results indicate that AFG transplantation exhibits reliable biocompatibility and effectiveness in promoting spinal cord repair in a non-human primate SCI model. Owing to the similarities in genetics and physiology between non-human primates and humans, AFG transplantation therapy is likely suitable for use in human spinal cord repair.

Keywords:
Aligned fibrin hydrogel; Lateral hemisection model; Non-human primate; Spinal cord injury repair

#Authors contributed equally.

***Corresponding authors:**
Guihuai Wang,
guihuai_wang@163.com;
Xiumei Wang,
wxm@mail.tsinghua.edu.cn

How to cite this article:
Yang J, Man W, Yang K, Cao Z, Ma C, Kim K, *et al.* Preclinical evaluation of aligned fibrin nanofibre hydrogels in a non-human primate model of spinal cord injury: A pilot study. *Biomater Transl.* 2025, 6(3), 334-344.

doi: 10.12336/bmt.24.00079

1. Introduction

Spinal cord injury (SCI) is a destructive event that leads to permanent motor, sensory, and autonomic deficits below the site of injury.[1] SCI affects approximately 760,000 patients worldwide each year and often occurs in young adults, posing significant economic and social burdens.[2] After SCI, the loss of neural tissue and secondary cascading damage lead to the formation of a cystic cavity and a fibrotic glial scar, which constitute formidable barriers to axon regeneration in the lesion site.[3] Current treatment options, including treatment with high doses of methylprednisolone and early decompressive surgery, have not achieved satisfactory clinical results.[4] Thus, the development of new therapeutic strategies focused on both axonal regeneration and functional neural circuit reconstruction is expected to be the future of SCI research.

Recently, biomaterial scaffold implantation as a potential strategy to repair the spinal cord after injury has received increasing attention, and there have been rapid advancements in materials science and engineering. For effective spinal cord regeneration, natural or synthetic biomaterial scaffolds can fill the cavity in the injured area and guide and support axonal growth and extension.[5] Moreover, a biomaterial scaffold-based platform containing stem cells and bioactive molecules could also serve as a combination strategy to facilitate neural repair by creating a regenerative niche.[6-8] The development of potent biomaterial scaffolds for clinical practice is a long-desired goal in regenerative medicine. While promising

laboratory results have been achieved with biomaterial scaffolds that are combined with cells or growth factors, only a few have successfully advanced to clinical trials.[9,10] These efforts face challenges related to complexity, biosafety, and the need for additional components such as stem cells or growth factors, which complicate their clinical translation. Consequently, the development of simplified, natural biomaterial scaffolds that promote endogenous repair while addressing biosafety concerns and eliminating the need for additional cellular components is vital for the successful clinical application of biomaterial scaffolds for SCI treatment.

Fibrin is a biodegradable, biocompatible, and bioactive natural polymer that has been approved by the U.S. Food and Drug Administration for intraoperative use in tissue repair.[11] In addition to their high biosafety characteristics, fibrin hydrogels have been extensively proven to promote nerve regeneration in the central nervous system.[5,12,13] Additionally, fibrin hydrogels can be designed to mimic the viscoelastic properties of human spinal cord tissue by adjusting the ratio of fibrinogen to thrombin via cross-linking reactions.[14,15] In the past decade, our group has developed a three-dimensional hierarchically aligned fibrin nanofibre hydrogel scaffold (AFG) and thoroughly studied its application for injured spinal cord repair and neural regeneration.[12,14,16-25] The highly orientated structure of the AFG subtly mimics the linearly ordered white matter of the spinal cord, which can support axonal regrowth parallel to the fibre bundles.[12,14,17] In addition, the appropriate mechanical properties (Young's modulus, ~1.5 kPa) and nanoscale topographical cues (nanofibre diameter, ~100 nm) endow AFGs with unique potential to closely interact with endogenous neural stem cells and promote subsequent endogenous nerve repair.[16,18] In our previous studies, the transplantation of AFGs facilitated axon regeneration and motor function recovery in rat and canine models of SCI, indicating the potential feasibility of AFG therapy in SCI clinical trials.[12,14,17,20,22,23] However, there are marked biological and physiological differences among different animal species, which should be considered, especially when this strategy is translated to the clinic. Thus, given the limitations of rodent and canine SCI models, establishing a reliable large animal model is crucial for solving these issues.

Compared to other species, non-human primates (NHPs) share closer genetic, physiological, neuroanatomical, and neurodevelopmental similarities with humans, making them an ideal preclinical model for developing promising potential therapies.[26] The complex biological processes that occur after SCI in NHPs most likely mirror those that occur in humans, which could provide unique insights to predict the biosafety and efficacy of spinal cord repair treatments that cannot be obtained by studying other organisms.[27] Furthermore, the size, surgical extent, and scaffold transplantation process are more similar in NHPs and humans, and the long lifespan of NHPs allows for the study of long-term outcomes following biomaterial scaffold implantation.[28-30] Thus, an NHP model is necessary to test the potential of AFG treatment for SCI repair, which lays the groundwork for translation into clinical trials.

The aim of this study was to explore the therapeutic potential of AFG implantation in an NHP model. Using Macaca fascicularis right–lateral hemisection SCI model mice with a 1-cm gap at the T9–T10 level, we sought to evaluate the neuroregenerative effects of the AFG and its ability to promote motor function recovery (**Figure 1A**). This research is expected to contribute critical preclinical evidence, facilitating the clinical translation of AFG therapy in SCI treatment.

2. Methods

2.1. Hydrogel preparation

The AFG was prepared by electrospinning as previously described.[18] The electrospinning solution was prepared from fibrinogen (Sigma Aldrich, St. Louis, MO, USA) dissolved in distilled water with polyethylene oxide (PEO, Sigma Aldrich) at 8 mg/mL. Under a voltage of 5 kV, the solution was continuously ejected at a speed of 3 mL/min and collected in a container filled with 4 U/mL thrombin (Sigma Aldrich) and a 50 mM CaCl2 liquid bath. The collection container was rotated at a speed of 50 r/min to ensure the alignment of the fibrin fibres. The electrospun fibrin fibres were collected to form bundles, sterilised in alcohol (75% w/v) under ultraviolet light, and washed with distilled water for further use.

2.2. Animal procedures

A total of four male Macaca fascicularis monkeys (9 years old, 7 ± 1 kg) were used in this study. The monkeys were individually bred and housed at Guangdong Landau Biotechnology Co. Ltd. (animal licence No. SYXK (Yue) 2018-0187), and the cages has an environmental temperature of 18–24°C and humidity level of 40–70%. The monkeys were also housed under a 12-hour light/dark cycle. All animal experiments were approved in advance by the Institutional Animal Care and Use Committee of Guangdong Landau Biotechnology Co. Ltd. and Guangdong Primate Research Centre (Guangzhou, China; approval No. G2ABR20200701; approval date: July 1, 2020). Animal surgery was performed under sterile conditions by three neurosurgeons at a surgical laboratory at Guangdong Landau Biotechnology Co. Ltd. This facility has obtained AAALAC International accreditation and a China National Accreditation Service for Conformity Assessment certificate (No. LA0018). The monkeys were randomly divided into two groups: the AFG graft group and the control group, with two monkeys in each group.

All monkeys underwent 12 hours of water and food deprivation and were anaesthetised via intramuscular injection of Zoletil 50 (Virbac S.A., Carros, France) at a dose

[1]State Key Laboratory of New Ceramics and Fine Processing, Key Laboratory of Advanced Materials, School of Materials Science and Engineering, Tsinghua University, Beijing, China; [2]Department of Neurosurgery, Beijing Tsinghua Changgung Hospital, School of Clinical Medicine, Tsinghua Medicine, Tsinghua University, Beijing, China; [3]Centre for Biomaterials and Regenerative Medicine, Wuzhen Laboratory, Tongxiang, Zhejiang Province, China; [4]Department of Neurosurgery, Beijing Chaoyang Hospital, Capital Medical University, Beijing, China

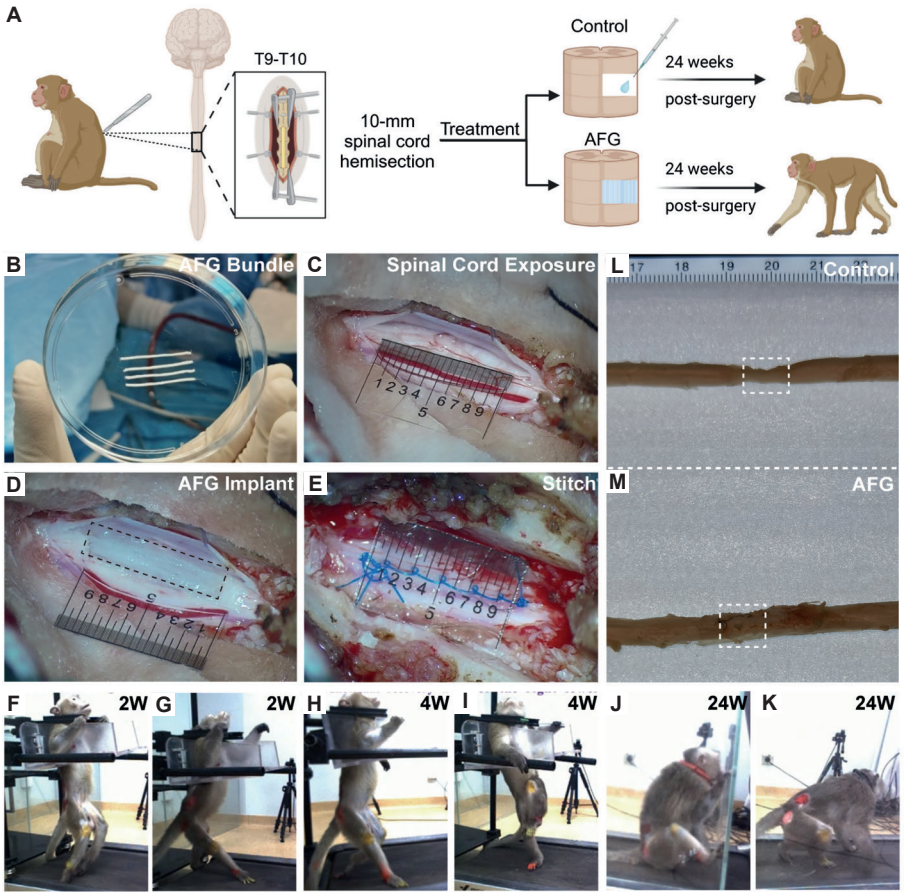

Figure 1. Overview of AFG treatment in cynomolgus monkeys with spinal cord injury. (A) Schematic illustration of the animal experiment evaluation. Created with BioRender.com. (B) Preparation of the AFG. (C–E) Surgical procedure: identification of the injury site, transplantation of the AFG, and suturing of the dura mater. (F–K) Observation of recovery of motor function. (L, M) Appearance of spinal cord tissue at 24 weeks after surgery. Rectangles indicate injured sites.
Abbreviation: AFG: Aligned fibrin nanofibre hydrogel scaffold.

of 5–8 mg/kg. Anaesthesia was maintained by isoflurane inhalation (1.5–2.0%) after tracheal intubation. Respiratory rate, heart rate, blood oxygen saturation, and blood pressure were monitored constantly during surgery. The monkeys were placed in a prone position, and the operation was guided by standard clinical surgical procedures. In brief, the T9 spinous was located under X-ray (Additional Figure 1), and a 6-cm skin incision was made at T9–T10 under sterile conditions. The subcutaneous tissue and paraspinal muscle were stripped laterally to expose the T9–T10 spinous and lamina, which were then removed using piezosurgery and rongeur to expose the dura mater, followed by a cut to the dura mater under a surgical microscope (Carl Zeiss, Oberkochen, Germany) to further expose the spinal cord for hemisection. The posterior median vessel of the spinal cord was electrocauterised, and a 1-cm lateral right half of the spinal cord was carefully transected using microscissors with intraoperative electrophysiological monitoring. After haemostasis, a total of 12 bundles of the AFG hydrogel (10 mm long and 0.5 mm diameter for each bundle) were transplanted to fill the surgical gap of each monkey in the AFG group, and the monkeys in the control group received only 1 mL of normal saline to fill the gap. After that, the dura mater, paraspinal muscle, subcutaneous tissue, and skin were sutured layer-by-layer. Each monkey received penicillin (15 mg/kg, intravenously, twice a day) to prevent postoperative infection.

For postoperative care, the wound site was cleaned with povidone iodine every day. The bladder was manually emptied twice a day to assist in micturition until recovery of the micturition reflex. When a pressure ulcer was observed on the skin, the pressure ulcer wound was immediately treated by debridement, povidone iodine cleansing, and dressing. Moreover, the hind limb muscles were massaged, and the major joints of the hip, knee, and ankle were passively flexed four times a day to prevent atrophy. After recovery for 2 months, the monkeys were allowed to walk daily for active exercise.

2.3. Behavioural assessment

A commercial primate behaviour analysis system (PrimateScan 1.0, CleverSys Inc., Reston, VA, USA) was used to evaluate the motor function and trajectory of each monkey.[29] Briefly, monkeys were placed in a transparent ambulation acrylic chamber (1.17 m × 1.2 m × 0.82 m) with continuous video recording for 90 minutes in a quiet room at 2, 4, 8, 12, 16, 20, and 24 weeks after surgery. The monkeys whose upper body was restrained were allowed to move freely with prior training (speed: 0.5 m/s), and reflective paint was applied to the shaved

skin of the anterior superior iliac spines, posterior superior iliac spines, knees joints, ankle joints, heels, and second metatarsophalangeal joints. The three-dimensional spatial coordinates of the reflective markers were recorded by multiple high-speed cameras (recording frequency: 100 Hz) and stored in a PrimateScan system (CleverSys, Inc.) while the monkeys were moving. The kinematics-based analyses of the monkeys were performed automatically by PrimateScan software Version 1.00 (CleverSys Inc.). The hindlimb was modelled as a series of rigid segments linked together, and the angles at the joints were calculated on the basis of this configuration.

2.4. Tissue harvesting and processing

Monkeys were anaesthetised with Zoletil 50 (8 mg/kg, intramuscular, Virbac S.A.), euthanised with intravenous sodium pentobarbital at 24 weeks post-surgery, and then transcardially perfused with 0.9% saline followed by cold 4% formaldehyde. The spinal cords from T9–T10 were quickly retrieved and fixed in 4% formaldehyde for another 48 hours at 4°C. The samples of spinal cords were subsequently dehydrated in a series of sucrose–phosphate-buffered saline (PBS) solutions with increasing sucrose concentrations (10%, 20%, and 30% w/v, 24 hours each, at 4°C). The harvested spinal cord tissues were then embedded in OCT compound (Tissue-Tek, Sakura Finetechnical Co., Tokyo, Japan) and serially longitudinally sliced into 10-μm-thick sections using a freezing microtome (CM1950, Leica Microsystems, Wetzlar, Germany).

2.5. Haematoxylin & eosin staining

For general histological assessment of the lesion site and adjacent tissue, the sections were air-dried at 37°C and washed with distill water. The sections were subsequently stained with haematoxylin (Sigma–Aldrich) for 9 minutes, rinsed with distill water, differentiated with 1% (v/v) alcoholic hydrogen chloride, and washed again with dH2O for 20 minutes. After counterstaining with eosin (Sigma–Aldrich) for 3 minutes, the sections were rinsed with increasing concentrations of ethanol (70%, 80%, 90%, 95%, 100%, and 100%) and xylene. The dehydrated sections were then coverslipped with neutral resin. Images were captured using a Pannoramic SCAN scanner (3DHIESTECH, Budapest, Hungary), and the images were processed using CaseCenter 2.9SP1 software (3DHIESTECH).

2.6. Immunofluorescence staining

The spinal cord sections were rinsed with PBS and blocked with 10% goat serum for 30 minutes at room temperature. Then, the sections were incubated with different primary antibodies (diluted in 0.3% Triton X-100 in PBS) overnight at 4°C. The tissue sections were washed three times with PBS and incubated with the indicated secondary antibodies for 1 hour at 37°C in the dark. The list of antibodies used in this study is presented in Additional Table 1. 4′,6-Diamidino-2-phenylindole-containing mounting medium (Abcam, Cambridge, UK) was used to stain the nuclei. Images were captured using a Zeiss Axio Scan Z1 slide scanner (Carl Zeiss) and processed using Zen 2.6 software (Carl Zeiss).

2.7. Statistical analysis

Immunofluorescence images were quantitatively analysed using ImageJ 1.51 k software (v1.52a; National Institutes of Health, Bethesda, MD, USA). Statistical graphs were generated using GraphPad Prism 7.0 (GraphPad Software, Boston, MA, USA, www.graphpad.com), and figures were assembled using Adobe Illustrator 22.1 (Adobe Inc., Austin, TX, USA).

3. Results

3.1. Overview of aligned fibrin nanofibre hydrogel scaffold treatment in cynomolgus monkeys with spinal cord injury

Before surgery, sterile AFG hydrogels were meticulously fabricated and shaped into 1 cm-long bundles (**Figure 1B**). A 1-cm-long defect was created on the right side of the spinal cord in four cynomolgus monkeys via precision microsurgical techniques (Additional Video 1). The lesion boundaries were precisely reconfirmed via a flexible ruler, with an emphasis on minimising collateral damage, notably to the posterior and anterior spinal arteries (**Figure 1C**). For the AFG-treated monkeys, the prepared AFG bundle was positioned at the lesion site, followed by thorough irrigation of the surgical site with saline and waterproof suturing (**Figure 1D** and **E**). Conversely, the control monkeys underwent only standard saline irrigation and waterproof suturing, without any supplementary interventions. Within 2 weeks post-surgery, monkeys exhibited identical symptoms of complete paralysis in their right lower limbs, resulting in their inability to maintain an upright stance. Additionally, as a result of potential underlying factors, including spinal shock and ischaemia, both monkeys displayed impaired motor function in their left hind limbs (**Figure 1F**, **G**, and Additional Videos 2, and 3). Four weeks post-surgery, partial restoration of motor function was noted in the bilateral lower limbs of both monkeys. Notably, only the AFG-treated monkeys demonstrated substantial motor recovery in the right hind limb (**Figure 1H** and **I**). After 24 weeks of follow-up, both monkeys showed continued improvement in motor function. However, only the AFG-treated monkeys achieved the milestone of being able to stand and walk independently, indicating a more favourable recovery trajectory (**Figure 1J** and **K**). Also, the harvested spinal cord tissues revealed that the AFG-treated monkeys presented significantly greater restoration of tissue integrity than did the control monkeys (**Figure 1L** and **M**). These results demonstrate the successful establishment of a NHP SCI model and provide preliminary evidence of the potential safety and effectiveness of AFG in SCI treatment.

3.2. Aligned fibrin nanofibre hydrogel scaffold improves the walking behaviour in cynomolgus monkeys with spinal cord injury

Kinematics-based analyses were applied to further quantitatively evaluate improvements in animal walking behaviour following AFG treatment. An initial observation of the effect of AFG treatment on walking behaviour following SCI can be obtained through the depiction of walking trajectories, as shown by the stick plots in **Figure 2A**.

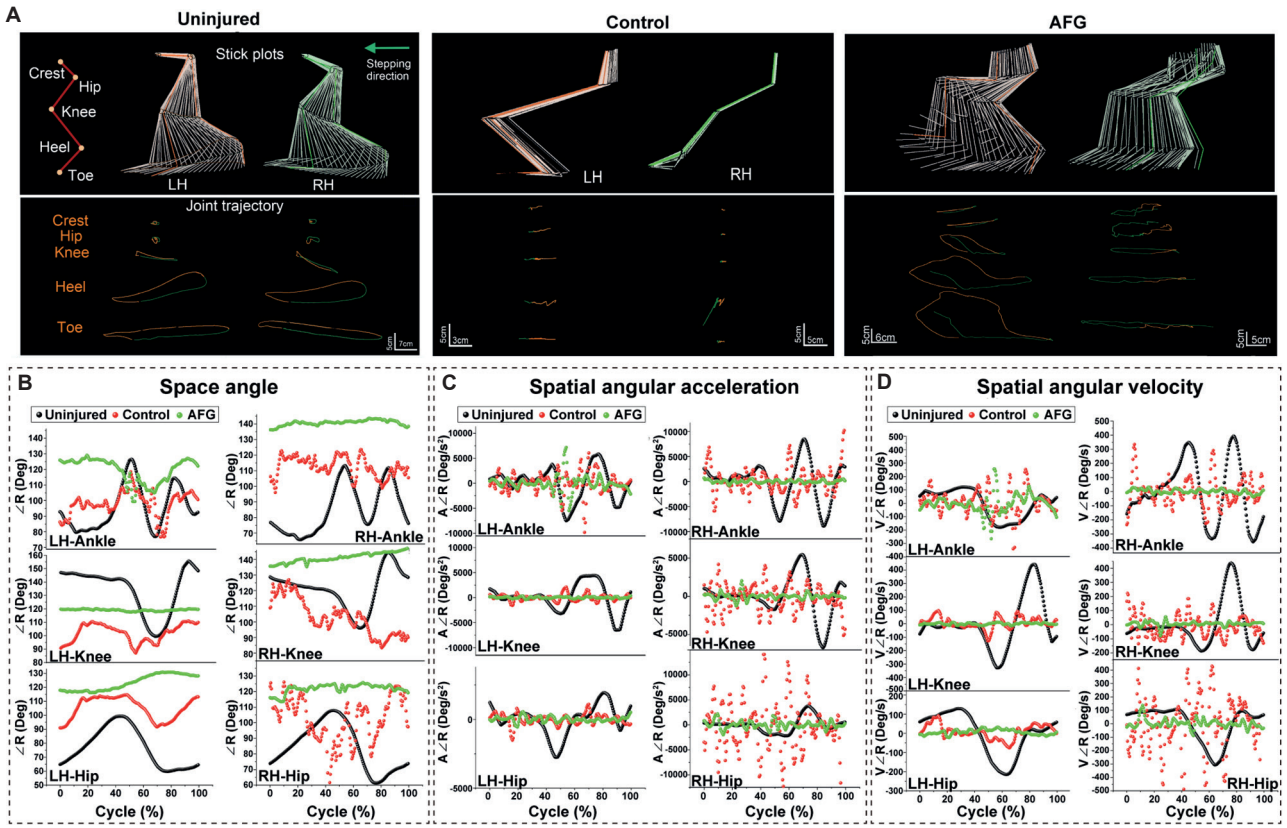

Figure 2. AFG improves the walking behaviour in cynomolgus monkeys with spinal cord injury using kinematics-based analyses. (A) Depiction of walking trajectories with stick plots. (B–D) Space angle, spatial angular acceleration, and spatial angular velocity of the ankle, knee, and hip joints.
Abbreviations: AFG: Aligned fibrin nanofibre hydrogel scaffold; LH: Left heel; RH: Right heel.

Before surgery, the animals exhibited rhythmic stepping with alternating left and right feet, resulting in normal gait patterns. Twenty-four weeks post-surgery, significant abnormalities in the trajectories of both lower limbs were evident in the control monkey, with a complete absence of a normal walking trajectory due to the injured side. In contrast, the AFG-treated monkeys exhibited normal walking trajectories, although they were still not fully restored to their preoperative condition. Furthermore, three parameters (i.e., space angle, spatial angular acceleration, and spatial angular velocity) were calculated for the ankle, knee, and hip joints to quantitatively assess the similarity of walking patterns across three distinct statuses (**Figure 2B–D**).

For the uninjured monkeys, all the parameters for all the joints exhibited periodic variations. For the AFG-treated monkeys, the angular variation trends of all joints in the left lower limb were similar to those of normal gait, and the trends in the right lower limb were also similar, albeit with less stability and continuity in the angular values. In contrast, for the control monkey, in addition to the ankle joint in the left lower limb showing a trend similar to that of the uninjured monkey, the parameters of the other joints lacked distinct periodic variations. These findings suggest that AFG treatment not only aids in the recovery of motor function on the injured side of monkeys with spinal cord injuries but also contributes to the preservation of function on the noninjured side.

3.3. Aligned fibrin nanofibre hydrogel scaffold improves the morphology of spinal cord tissue in cynomolgus monkeys with spinal cord injury

To further confirm that AFG treatment promotes histological repair in injured spinal cords, haematoxylin and eosin staining and immunofluorescence staining were employed to observe histopathological changes at 24 weeks post-surgery. As illustrated in **Figure 3**, within the core injury area of the spinal cord tissue of the control monkeys, obvious cavities formed, devoid of any newly grown tissue. Limited loose tissue was also present in the areas adjacent to both the proximal and distal ends, as well as in the peripheral zones surrounding the core injury area. Notably, there was a discernible trend for these spinal cord cavities to enlarge towards the contralateral, uninjured area. Conversely, in the injured area of the monkey that had undergone AFG treatment, no significant cavity formation was observed. The newly formed tissue closely resembled that of the uninjured spinal cord, displaying prominent features of directionally arranged structures. Similarly, the contralateral spinal cord tissue exhibited good continuity and no notable differences compared with normal spinal cord tissue.

We further characterised the similarity between the newly formed tissue and neural tissue within the injured area by using glial fibrillary acidic protein (GFAP) and β-tubulin III as markers for astrocytes and neurons, respectively. As shown in **Figure 4** and Additional Figure 2, within the core region

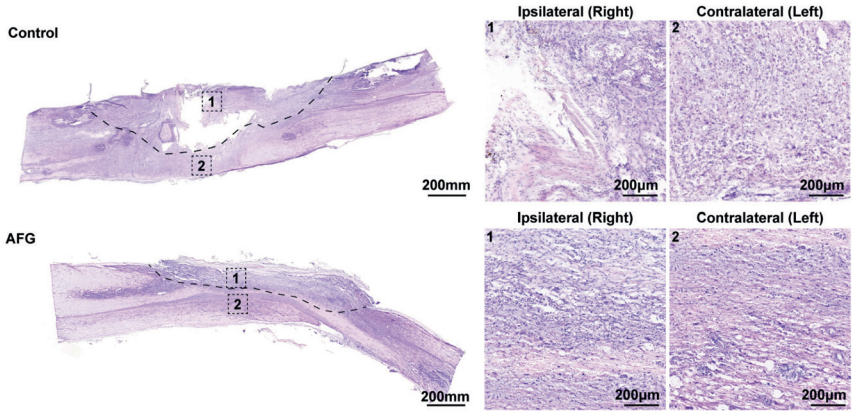

Figure 3. AFG improves the morphology of spinal cord tissue in cynomolgus monkeys with spinal cord injury using haematoxylin and eosin staining. In the control monkeys, extensive cavity formation was observed in the injured area, accompanied by minimal tissue regeneration. In contrast, AFG-treated monkeys presented minimal cavity formation, with newly formed tissue closely resembling the normal spinal cord and exhibiting good continuity. Enlarged views of representative fields 1 and 2 within the lesion area and in the adjacent counterparts are shown in the right panels. The dotted lines delineate the interface between morphologically abnormal tissues and their adjacent relatively normal counterparts. Scale bars: 200 mm (left), 200 μm (right).
Abbreviation: AFG: Aligned fibrin nanofibre hydrogel scaffold.

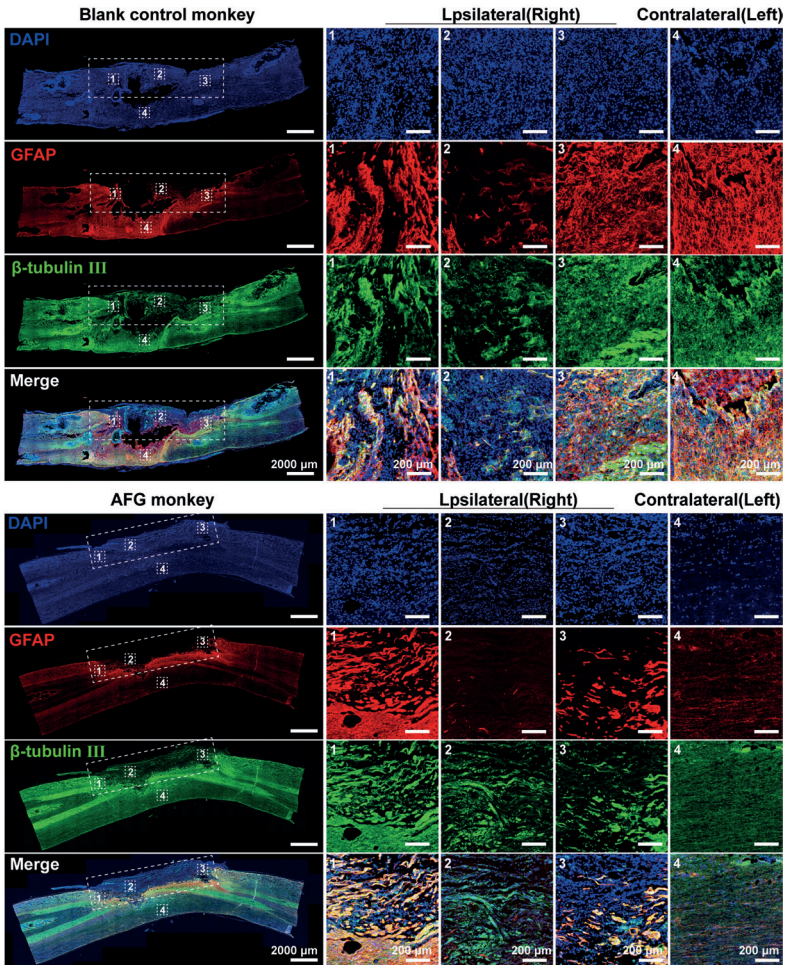

Figure 4. AFG increases the expression of GFAP and β-tubulin III in spinal cord tissue in cynomolgus monkeys with spinal cord injury using immunofluorescence staining. The control monkey tissues exhibited disorganised and minimal β-tubulin III expression, along with diffuse and irregular GFAP expression in the lesion core. In contrast, the AFG-treated monkey tissues presented aligned β-tubulin III expression and a more structured GFAP distribution, indicating enhanced neural regeneration and better tissue organisation. Enlarged views of representative fields 1–3 within the lesion area (corresponding to the rostral, central, and caudal parts of the injury, respectively) and field 4 within the adjacent regions are shown in the right panels. The dotted rectangles indicate injured sites.
Abbreviations: AFG: Aligned fibrin nanofibre hydrogel scaffold; GFAP: Glial fibrillary acidic protein.

of the spinal cord defects in the control monkeys, despite the aggregation of numerous cells, GFAP and β-tubulin III were present in small amounts in the tissue. This finding indicates that the tissue growing in the central area of the injury area is a mixture of scattered, minimal neural tissue and a substantial amount of non-neural tissue. In contrast, within the injured areas of the AFG monkeys, in addition to a small amount of GFAP expression, a significant amount of β-tubulin III expression with an aligned cell arrangement was observed, suggesting notable neural regeneration in the core region of the injury. Although both monkeys exhibited extensive expression of GFAP and β-tubulin III, only the tissues of the AFG-treated monkeys displayed a clearly aligned cell arrangement. Additionally, the arrangement of GFAP- and β-tubulin III-positive cells on the uninjured side of both monkeys also differed.

We further observed the formation of myelinated nerve fibres in both monkeys by using neurofilament 200 (NF200) and myelin basic protein (MBP) as markers for axonal proteins and myelin sheaths, respectively (**Figure 5** and Additional Figure 3). In the control monkeys, the centre and both ends of the injured spinal cord exhibited scattered NF200-positive and MBP-positive cells. In contrast, the AFG-treated monkeys presented a greater abundance of filamentous, aligned NF200-positive cells, accompanied by some scattered MBP-positive cells, both at the injury centre and at the injury ends. Notably, there was strong colocalisation of MBP-positive and NF200-positive cells in the AFG-treated monkeys. Additionally, we costained for the vascular marker endothelial cell antigen 1 (RECA-1) and the neuronal outgrowth marker growth-associated protein 43 (GAP43) to investigate the growth of nerves and blood vessels during the regeneration process (**Figure 6** and Additional Figure 4). Compared with control monkeys, AFG-treated monkeys presented a greater number of RECA-1- and GAP43-positive cells at the injured site, with both cell types displaying improved alignment.

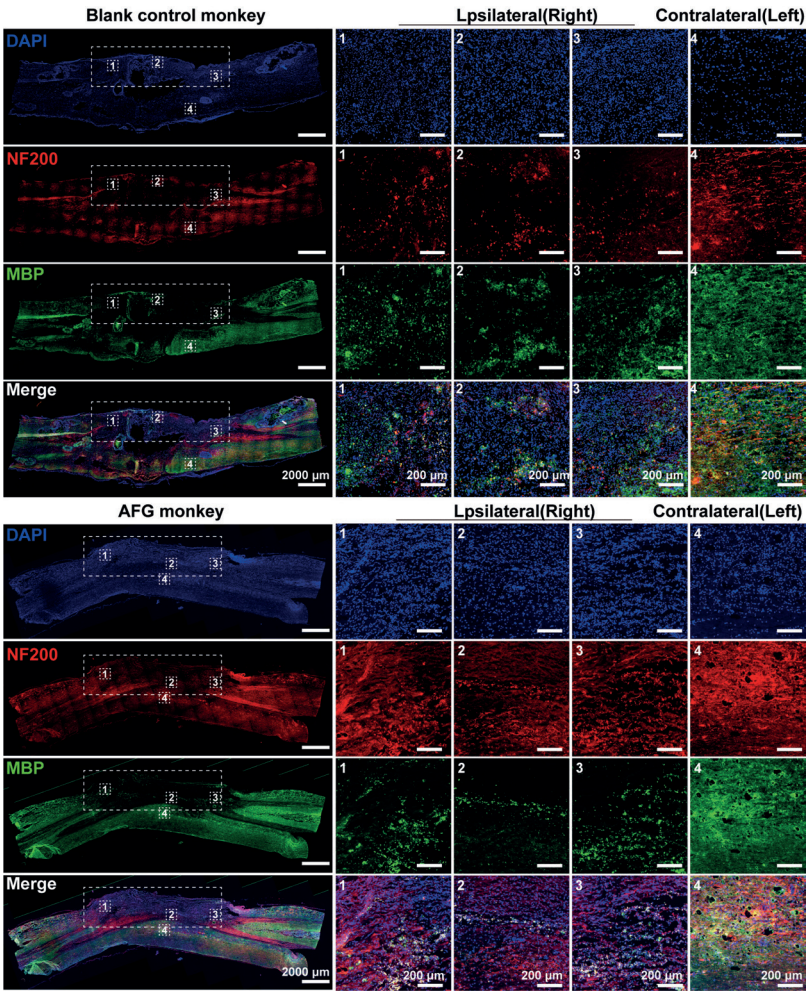

Figure 5. AFG increases the colocalisation of MBP and NF200 in spinal cord tissue in cynomolgus monkeys with spinal cord injury using immunofluorescence staining. Control monkeys presented scattered NF200- and MBP-positive cells at the centre and edges of the injured area. In contrast, AFG-treated monkeys presented a greater abundance of filamentous, aligned NF200-positive cells and some scattered MBP-positive cells, indicating improved axonal regeneration. The strong colocalisation of MBP- and NF200-positive cells in the AFG-treated monkeys suggested enhanced myelination in the injured area. Enlarged views of representative fields 1–3 within the lesion area (corresponding to the rostral, central, and caudal parts of the injury, respectively) and field 4 within the adjacent regions are shown in the right panels. The dotted rectangles indicate injury sites.
Abbreviations: AFG: Aligned fibrin nanofibre hydrogel scaffold; MBP: Myelin basic protein; NF200: Neurofilament 200.

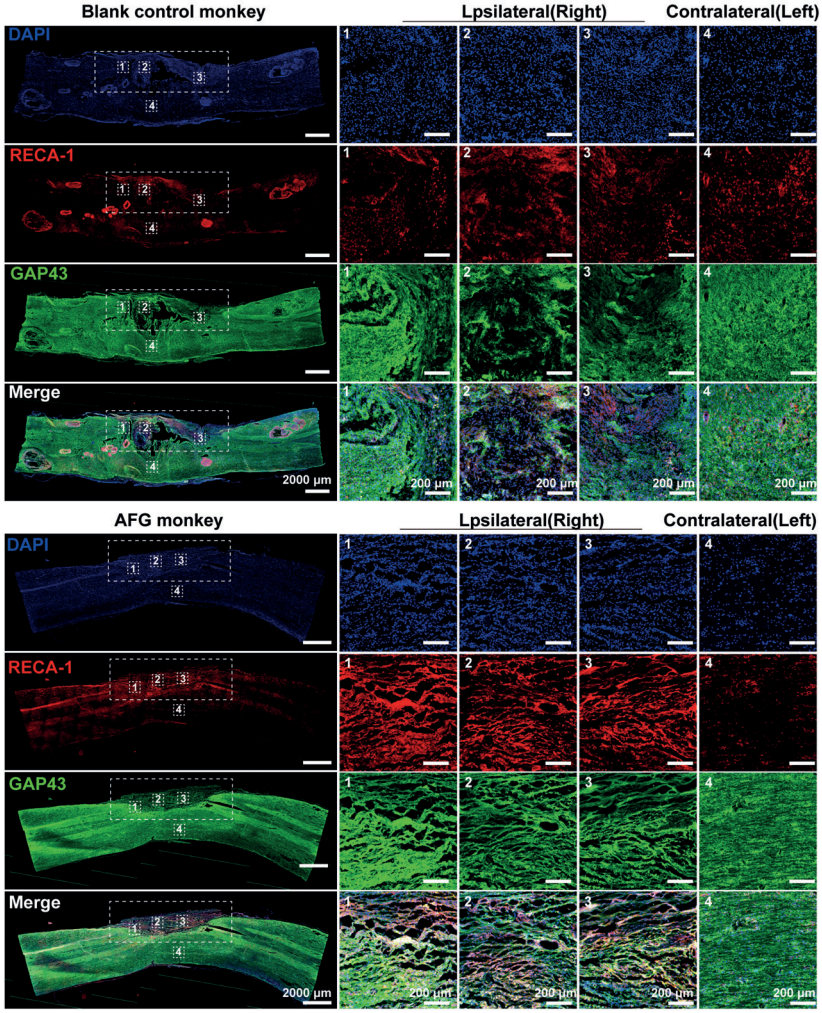

Figure 6. AFG increases the expression of RECA-1 and GAP43 in spinal cord tissue in cynomolgus monkeys with spinal cord injury using immunofluorescence staining. Compared with control monkeys, AFG-treated monkeys presented a greater density of RECA-1-positive and GAP43-positive cells at the injury site, with both cell types showing increased alignment. These findings suggest enhanced vascularisation and neuronal outgrowth during the regeneration process in AFG-treated monkeys. Enlarged views of representative fields 1–3 within the lesion area (corresponding to the rostral, central, and caudal parts of the injury, respectively) and field 4 within the adjacent regions are shown in the right panels. The dotted rectangles indicate injured sites.
Abbreviations: AFG: Aligned fibrin nanofibre hydrogel scaffold; GAP43: Growth-associated protein 43; RECA-1: Endothelial cell antigen 1.

In summary, morphological analyses demonstrated the effects of AFG treatment on spinal cord injuries in NHPs. AFG not only promotes the regeneration of neuronal axons in the injured area but also facilitates remyelination and vascularisation. Furthermore, AFG treatment promoted the aligned arrangement of newly formed tissues, which more closely resembled normal neural tissue. These findings highlight the potential of AFG as a therapeutic agent for repairing the injured spinal cord.

4. Discussion

We previously developed a novel implantable scaffold, the AFG. Fibrin, formed through the enzymatic interaction between fibrinogen and thrombin, has shown considerable potential for tissue implantation because of its complete biodegradability and excellent biocompatibility. Fabricated using the liquid-bath electrospinning method, the AFG features a highly aligned, hierarchically structured nanofibrous matrix with diameters ranging from 100 to 200 nm, providing precise anisotropic guidance for cytoskeletal elongation and the modulation of cellular behaviour. Additionally, owing to its substrate stiffness and neural tissue-like viscoelasticity, the AFG demonstrates promising neuroregenerative properties. In our previous studies, we showed that the AFG significantly promotes spinal cord repair in rodent and canine SCI models.[14,17,23] However, owing to the significant species differences between these animals and humans, the repair processes of SCI differ substantially. Thus, we cannot directly translate rodent and canine SCI treatment strategies to humans. Research in NHPs has become indispensable in advancing AFG towards clinical translation.[31] In the present study, we further evaluated the effect of AFG on spinal cord repair by using a NHP SCI model. We established a 10-mm hemisected spinal cord defect at the T9–T10 level in Macaca fascicularis monkeys. Within 24 weeks of follow-up, AFG implantation in situ triggered robust neural tissue regeneration and promoted motor function recovery.

This pilot study provides preclinical evidence for its potential translational application.

Despite numerous studies reporting the efficacy of various scaffolds in rodent models, only approximately 10 registered clinical trials can be found on Clinicaltrials.gov.[32] This highlights the significant challenges faced in translating biological scaffolds for SCI treatment into clinical practice. The primary underlying reason for this translational difficulty is species differences. First, owing to the vast size discrepancy between the human and rodent spinal cords, the severity of SCI in humans is substantially greater than that in rodent models, leading to different demands for the regenerative capacity of the spinal cord postinjury. Furthermore, many studies have demonstrated physiological differences between rodents and humans following SCI. While both species exhibit inflammation and demyelination, these effects are generally less severe in humans, with slower axonal degeneration and a more extensive Schwann cell response and cystformation.[33] Additionally, rodents have more extensive glial scarring with chondroitin sulfate proteoglycans, whereas humans have less extensive glial scarring, with chondroitin sulfate proteoglycans located primarily in blood vessels. These species-specific variations may have notable impacts on the integration efficiency and functionality of the biological scaffolds employed in the treatment of SCI.[34] Notably, nearly all scaffolds that have progressed to clinical trials have undergone prior research in NHP models, emphasising the importance of NHP research in bridging the gap between preclinical and clinical studies and enhancing the translational potential of AFG for injured spinal cord repair.

Although large hemisected spinal cord defects are less common clinically than contusion lesions are, they offer distinct advantages in assessing treatment efficacy in SCI studies. The extensive defect completely disconnects the ascending and descending tracts on one side, preventing the pseudofunctional recovery often observed in incomplete contusion models.[35] In our study, the animals exhibited complete motor dysfunction on the injured side for at least 8 weeks post-surgery, confirming the success of our model. Moreover, the hemisection model offers superior reproducibility by minimising variations in the injury area, which are common in contusion models despite careful parameter control. The surgical procedure in the present study also closely replicated clinical spinal cord surgery, emphasising vascular protection and waterproof dura mater suturing. The importance of the hemisection model is further underscored by its frequent application in SCI research. In recent decades, the neurotrophin-3-chitosan model has been the most commonly used model in macaque studies,[28,36] including milestone research, such as that of Rao *et al.*[28] conducted in 2018, which demonstrated that NT3-chitosan enables de novo regeneration and functional recovery in monkeys after SCI. Although functional compensation on the contralateral side is a concern, similar issues are present in contusion models, which may involve even more complex compensatory mechanisms in long-term studies. Additionally, while contusion models better mimic clinical SCI, treatments involving implantable hydrogels typically require surgical removal of scar tissue to prepare a graft bed, effectively converting the injury into a partial resection model.[37] In this context, the hemisection model better reflects this clinical scenario. Complete transection models, while avoiding compensatory effects, often lead to severe paralysis and potential complications such as pressure sores, urinary tract infections, and lower limb thrombosis, thereby posing significant ethical risks. Overall, the hemisection model provides a balance between experimental rigour and clinical relevance, making it an ideal choice for evaluating the effects of the AFG in SCI treatment.

In this study, we investigated the efficacy of AFG in treating SCI in NHPs by exploring both motor function recovery and tissue repair. Consistent with previous findings in rats and dogs, the AFG had a significant effect on motor function recovery in primate SCI models. At the end of the follow-up, the control monkey was unable to stand, whereas the AFG-treated monkey exhibited the ability to stand and walk independently, indicating a qualitative improvement in their quality of life. Notably, the motor function of the contralateral limb in the AFG-treated monkeys nearly returned to normal, whereas it remained partially impaired in the control monkeys. This finding suggests that AFG not only facilitates functional reconstruction of the injured spinal cord but also may mitigate the occurrence of secondary injuries, thereby inhibiting the expansion of the injury area and preserving residual tissue.

Histological analysis further demonstrated the multifaceted therapeutic effects of AFG in NHPs. Consistent with previous findings in rodent and canine models, AFG effectively mitigated cavity formation, as evidenced by haematoxylin & eosin staining, while promoting axonal regeneration and remyelination (β-tubulin III and NF200 expression). The colocalisation of NF200 and MBP confirmed enhanced remyelination, and the upregulation of GAP43 and RECA-1 further highlighted its role in promoting revascularisation of regenerating neural tissue. These findings collectively underscore the potential of the AFG to support both structural and functional repair in injured spinal cord tissues, which aligns with its observed motor functional benefits. The favourable performance of AFG in NHP SCI models provides confidence in advancing its clinical application, underscoring the translational potential of AFG for treating SCI in humans.

Notably, the sample size was relatively small. Since this was the first time that the AFG was used to treat SCI, ethical considerations required a limited number of animals per group in this pilot study, making it challenging to conclusively determine whether differences between the AFG-treated monkeys and the control monkeys were due to individual variations. Despite these constraints, this study has laid the groundwork for future research, and we aim to increase the sample size in subsequent studies to better understand the effectiveness of AFG. Another potential limitation is the scarcity of evaluation methods utilised. While behavioural recovery is the ultimate goal and most important outcome of AFG treatment, the lack of electrophysiological assessments, MRI scans, and other evaluative techniques has hindered our ability to fully characterise the effects of the AFG at different stages of the disease process. Specifically, the absence of electrophysiological assessments and in vivo imaging techniques has limited our ability to gain deeper insights into the effects of

AFG at various recovery stages and substantiate the observed behavioural findings. This limitation will be addressed in future studies with larger sample sizes. Additionally, unlike humans, monkeys cannot undergo systematic rehabilitation training after surgery. The lack of rehabilitation training may have significantly contributed to the limited recovery observed in both monkeys, which could have resulted in different outcomes when the study results were applied to clinical research.

5. Conclusions

In conclusion, this pilot study demonstrated the potential of the AFG to promote spinal cord repair in NHPs, bridging the gap between preclinical research and clinical application. AFG implantation led to robust neural tissue regeneration, significant motor function recovery, and tissue repair, which is consistent with prior findings in rodent and canine models. While limitations such as a small sample size, insufficient evaluation methods, and a lack of rehabilitation training warrant further investigation, these results provide valuable preclinical evidence supporting the translational potential of the AFG for treating SCI in humans. Additionally, future studies with larger cohorts and comprehensive evaluations are essential to advance AFG treatment towards clinical application.

Acknowledgement
The authors thank Junhua Rao and colleagues from Guangdong Landau Biotechnology Co. Ltd for the help of animal experiments.
Financial support
This study was financially supported by the National Natural Science. Foundation of China (Nos. 32271414, 82201521, 82301560), the Tsinghua. Precision Medicine Foundation (No. 2022TS001), the Beijing Natural Science. Foundation (Nos. 7242187, 2254091), and State Key Laboratory of New Ceramic Materials Tsinghua University (No. KF202409).
Conflicts of interest statement
The authors declare that there are no conflicts of interest.
Author contributions
Conceptualization: JY, GW, and XW; *Data curation:* JY and GW; *Formal analysis:* JY, ZC, CM, ZM, YL, YY, JZ, ZW, KK, and XW; *Funding acquisition:* WM, KY, GW, and XW; *Investigation:* JY, ZC, CM, and KK; *Methodology:* JY, ZC, CM, ZM, YL, YY, JZ, ZW, KK, and XW; *Project administration:* WM, KY, ZM, YL, YY, JZ, ZW, YL, XZ, and XW; *Software:* WM and KY; *Validation:* ZM, YL, YY, JZ, and ZW; *Visualization:* WM, KY, ZC, and CM; *Writing – original draft:* JY; *Writing – review & editing:* JY, WM, KY, and XW. All authors approved the final version of the manuscript.
Ethics approval and consent to participate
All animal experiments were approved in advance by the Institutional Animal Care and Use Committee of Guangdong Landau Biotechnology Co. Ltd. and Guangdong Primate Research Centre (Guangzhou, China; approval No. G2ABR20200701; approval date: July 1, 2020).
Consent for publication
Not applicable.
Availability of data
Not applicable.

References

1. Lu Y, Shang Z, Zhang W, *et al.* Global incidence and characteristics of spinal cord injury since 2000-2021: A systematic review and meta-analysis. *BMC Med.* 2024;22:285. doi: 10.1186/s12916-024-03514-9
2. Kumar R, Lim J, Mekary RA, *et al.* Traumatic spinal injury: Global epidemiology and worldwide volume. *World Neurosurg.* 2018;113:e345-e363. doi: 10.1016/j.wneu.2018.02.033
3. Tran AP, Warren PM, Silver J. The biology of regeneration failure and success after spinal cord injury. *Physiol Rev.* 2018;98:881-917. doi: 10.1152/physrev.00017.2017
4. Shah M, Peterson C, Yilmaz E, Halalmeh DR, Moisi M. Current advancements in the management of spinal cord injury: A comprehensive review of literature. *Surg Neurol Int.* 2020;11:2. doi: 10.25259/SNI_568_2019
5. Shen H, Fan C, You Z, Xiao Z, Zhao Y, Dai J. Advances in biomaterial-based spinal cord injury repair. *Adv Funct Mater.* 2022;32:2110628. doi: 10.1002/adfm.202110628
6. Lee CY, Chooi WH, Ng SY, Chew SY. Modulating neuroinflammation through molecular, cellular and biomaterial-based approaches to treat spinal cord injury. *Bioeng Transl Med.* 2023;8:e10389. doi: 10.1002/btm2.10389
7. Yang J, Yang K, Man W, *et al.* 3D bio-printed living nerve-like fibers refine the ecological niche for long-distance spinal cord injury regeneration. *Bioact Mater.* 2023;25:160-175. doi: 10.1016/j.bioactmat.2023.01.023
8. Yang J, Kim K, Liu Y, *et al.* 3D bioprinted dynamic bioactive living construct enhances mechanotransduction-assisted rapid neural network self-organization for spinal cord injury repair. *Bioact Mater.* 2025;46:531-554. doi: 10.1016/j.bioactmat.2024.12.028
9. Tang F, Tang J, Zhao Y, *et al.* Long-term clinical observation of patients with acute and chronic complete spinal cord injury after transplantation of NeuroRegen scaffold. *Sci China Life Sci.* 2022;65:909-926. doi: 10.1007/s11427-021-1985-5
10. Xiao Z, Tang F, Zhao Y, *et al.* Significant improvement of acute complete spinal cord injury patients diagnosed by a combined criteria implanted with neuroregen scaffolds and mesenchymal stem cells. *Cell Transplant.* 2018;27:907-915. doi: 10.1177/0963689718766279
11. Spotnitz WD. Fibrin sealant: Past, present, and future: A brief review. *World J Surg.* 2010;34:632-634. doi: 10.1007/s00268-009-0252-7
12. Yang K, Yang J, Man W, *et al.* N-cadherin-functionalized nanofiber hydrogel facilitates spinal cord injury repair by building a favorable niche for neural stem cells. *Adv Fiber Mater.* 2023;5:1349-1366. doi: 10.1007/s42765-023-00272-w
13. Yu Z, Li H, Xia P, *et al.* Application of fibrin-based hydrogels for nerve protection and regeneration after spinal cord injury. *J Biol Eng.* 2020;14:22. doi: 10.1186/s13036-020-00244-3
14. Yao S, Yu S, Cao Z, *et al.* Hierarchically aligned fibrin nanofiber hydrogel accelerated axonal regrowth and locomotor function recovery in rat spinal cord injury. *Int J Nanomedicine.* 2018;13:2883-2895. doi: 10.2147/IJN.S159356
15. Karimi A, Shojaei A, Tehrani P. Mechanical properties of the human spinal cord under the compressive loading. *J Chem Neuroanat.* 2017;86:15-18. doi: 10.1016/j.jchemneu.2017.07.004
16. Chai Y, Zhao H, Yang S, *et al.* Structural alignment guides oriented migration and differentiation of endogenous neural stem cells for neurogenesis in brain injury treatment. *Biomaterials.* 2022;280:121310. doi: 10.1016/j.biomaterials.2021.121310
17. Cao Z, Man W, Xiong Y, *et al.* White matter regeneration induced by aligned fibrin nanofiber hydrogel contributes to motor functional recovery in canine T12 spinal cord injury. *Regen Biomater.* 2022;9:rbab069. doi: 10.1093/rb/rbab069
18. Yao S, Liu X, Yu S, *et al.* Co-effects of matrix low elasticity and aligned topography on stem cell neurogenic differentiation and rapid neurite outgrowth. *Nanoscale.* 2016;8:10252-10265. doi: 10.1039/c6nr01169a
19. Du J, Liu J, Yao S, *et al.* Prompt peripheral nerve regeneration induced

by a hierarchically aligned fibrin nanofiber hydrogel. *Acta Biomater.* 2017;55:296-309.
doi: 10.1016/j.actbio.2017.04.010

20. Yao S, He F, Cao Z, *et al.* Mesenchymal stem cell-laden hydrogel microfibers for promoting nerve fiber regeneration in long-distance spinal cord transection injury. *ACS Biomater Sci Eng.* 2020;6:1165-1175. doi: 10.1021/acsbiomaterials.9b01557
21. Yang S, Zhu J, Lu C, *et al.* Aligned fibrin/functionalized self-assembling peptide interpenetrating nanofiber hydrogel presenting multi-cues promotes peripheral nerve functional recovery. *Bioact Mater.* 2022;8:529-544. doi: 10.1016/j.bioactmat.2021.05.056
22. Man W, Yang S, Cao Z, *et al.* A multi-modal delivery strategy for spinal cord regeneration using a composite hydrogel presenting biophysical and biochemical cues synergistically. *Biomaterials.* 2021;276:120971. doi: 10.1016/j.biomaterials.2021.120971
23. Cao Z, Yao S, Xiong Y, *et al.* Directional axonal regrowth induced by an aligned fibrin nanofiber hydrogel contributes to improved motor function recovery in canine L2 spinal cord injury. *J Mater Sci Mater Med.* 2020;31:40. doi: 10.1007/s10856-020-06375-9
24. Yang CY, Meng Z, Yang K, *et al.* External magnetic field non-invasively stimulates spinal cord regeneration in rat via a magnetic-responsive aligned fibrin hydrogel. *Biofabrication.* 2023;15:035022. doi: 10.1088/1758-5090/acdbec
25. Kim K, Yang J, Li C, *et al.* Anisotropic structure of nanofiber hydrogel accelerates diabetic wound healing via triadic synergy of immune-angiogenic-neurogenic microenvironments. *Bioact Mater.* 2025;47:64-82. doi: 10.1016/j.bioactmat.2025.01.004
26. Wu J, Shi Y, Yang S, *et al.* Current state of stem cell research in non-human primates: An overview. *Med Rev (2021).* 2023;3:277-304. doi: 10.1515/mr-2023-0035
27. Courtine G, Bunge MB, Fawcett JW, *et al.* Can experiments in nonhuman primates expedite the translation of treatments for spinal cord injury in humans? *Nat Med.* 2007;13:561-566. doi: 10.1038/nm1595
28. Rao JS, Zhao C, Zhang A, *et al.* NT3-chitosan enables de novo regeneration and functional recovery in monkeys after spinal cord injury. *Proc Natl Acad Sci U S A.* 2018;115:E5595-E5604. doi: 10.1073/pnas.1804735115
29. Zeng X, Wei QS, Ye JC, *et al.* A biocompatible gelatin sponge scaffold confers robust tissue remodeling after spinal cord injury in a non-human primate model. *Biomaterials.* 2023;299:122161. doi: 10.1016/j.biomaterials.2023.122161
30. Han S, Yin W, Li X, *et al.* Pre-clinical evaluation of CBD-NT3 modified collagen scaffolds in completely spinal cord transected non-human primates. *J Neurotrauma.* 2019;36:2316-2324. doi: 10.1089/neu.2018.6078
31. Tsintou M, Dalamagkas K, Makris N. Advancing research in regeneration and repair of the motor circuitry: Non-human primate models and imaging scales as the missing links for successfully translating injectable therapeutics to the clinic. *Int J Stem Cell Res Ther.* 2016;3:042. doi: 10.23937/2469-570X/1410042
32. Hyun JK, Kim HW. Clinical and experimental advances in regeneration of spinal cord injury. *J Tissue Eng.* 2010;2010:650857. doi: 10.4061/2010/650857
33. Chen H, Wang W, Yang Y, *et al.* A sequential stimuli-responsive hydrogel promotes structural and functional recovery of severe spinal cord injury. *Biomaterials.* 2025;316:122995. doi: 10.1016/j.biomaterials.2024.122995
34. Hagg T, Oudega M. Degenerative and spontaneous regenerative processes after spinal cord injury. *J Neurotrauma.* 2006;23:264-280. doi: 10.1089/neu.2006.23.263
35. Nemati SN, Jabbari R, Hajinasrollah M, *et al.* Transplantation of adult monkey neural stem cells into a contusion spinal cord injury model in rhesus macaque monkeys. *Cell J.* 2014;16:117-130.
36. Poulen G, Perrin FE. Advances in spinal cord injury: Insights from non-human primates. *Neural Regen Res.* 2024;19:2354-2364. doi: 10.4103/NRR.NRR-D-23-01505
37. Zhao Y, Tang F, Xiao Z, *et al.* Clinical study of neuroregen scaffold combined with human mesenchymal stem cells for the repair of chronic complete spinal cord injury. *Cell Transplant.* 2017;26:891-900. doi: 10.3727/096368917X695038

Received: October 28, 2024
Revised: January 27, 2025
Accepted: March 15, 2025
Available online: September 22, 2025